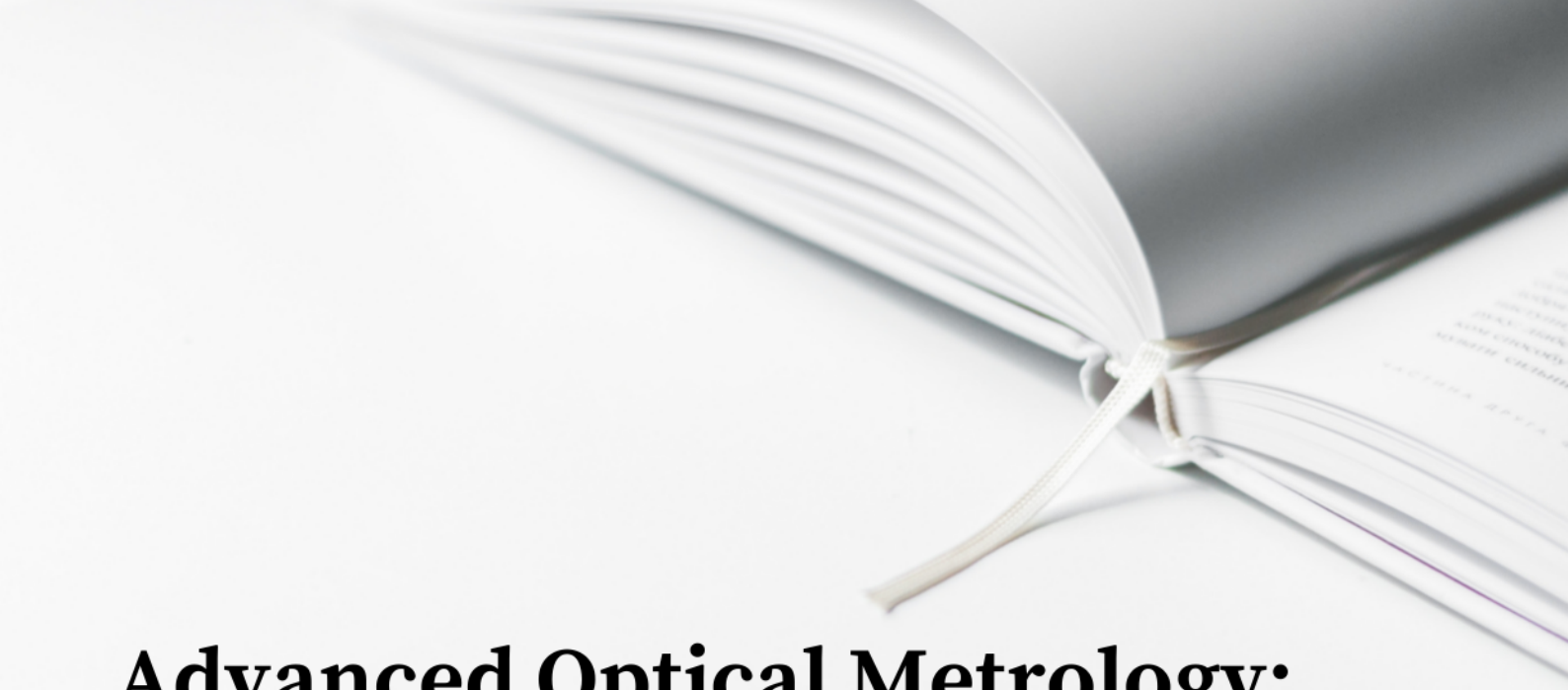

Advanced Optical Metrology: Geoscience now available

Geoscience is the scientific study of the Earth — more precisely, the study of the materials, structures, evolution, and dynamics of the Earth, including its organisms, natural minerals, and energy resources.

Geoscientists employ many analytical techniques to characterize these materials and samples — among them X-ray analytical techniques such as X-ray fluorescence (XRF) and X-ray diffractometry (XRD).

This eBook provides you with recent articles on the use of portable X-ray fluorescence (XRF) in combination with other methods for the characterization of the geochemistry of soils and sediments.

Download it now

This eBook is sponsored by OLYMPUS

WILEY

Received: 10 February 2021 | Revised: 28 May 2021 | Accepted: 6 July 2021

DOI: 10.1002/xrs.3254

SPECIAL ISSUE ARTICLE

X-RAY SPECTROMETRY WILEY

Recent developments of X-ray absorption spectroscopy as analytical tool for biological and biomedical applications

Ana Guilherme Buzanich

Department of Materials Chemistry, Division Structure Analysis, Federal Institute for Materials Research and Testing (BAM), Berlin, Germany

Correspondence
Ana Guilherme Buzanich, Department of Materials Chemistry, Division Structure Analysis, Federal Institute for Materials Research and Testing (BAM), Richard-Willstaetter-Strasse 11, 12489 Berlin, Germany.
Email: ana.buzanich@bam.de

X-ray absorption spectroscopy (XAS), in its various modalities, has gained exponential attention and applicability in the field of biological and biomedical systems. Particularly in this field, challenges like low concentration of analyte or proneness to radiation damage have certainly settle the basis for further analytical developments, when using X-ray based methods. Low concentration calls for higher sensitivity—by increasing the detection limits (DL); while susceptibility for radiation damage requires shorter measurement times and/or cryogenic sample environment possibilities. This manuscript reviews the latest analytical possibilities that make XAS more and more adequate to investigate biological or biomedical systems in the last 5 years.

1 | INTRODUCTION, CHALLENGES, AND PERSPECTIVES

When it comes to investigating biological and biomedical samples, yet the minute concentration of inorganic part plays a vital role, as it contributes to essential functions in these systems. The d-block elements of the periodic table play a decisive catalytic role in metalloproteins, which in turn are involved in many key biological processes—for example, oxygen transport and metabolism. Gaining information about local atomic and electronic structure of these metal ions allows us to get insight of the occurring processes, as this changes significantly.[1] This complex interplay between d-block metal ions and the biological process is defined as metallomics. In this context, X-ray based methods have gained exponential importance, in aiding the clarification by elemental imaging analysis of accumulated metal species and metal-containing compounds in biological materials, as presented by Collingwood and Adams.[2] Not just the amount of metal species but also the species itself in its local coordination environment is important to extract structure–property relationship.

X-ray absorption spectroscopy (XAS) offers such answers, which aid obtaining structure–property relationships, also as a tool for speciation imaging. XAS in its numerous modii has unique valences, such as element specificity, probing electronic structure, or environment changes in the vicinity of the studied element, with subatomic resolution (0.1 Å). For the novice investigators in this field, a tutorial highlighting the features and examples in biological and biomedical applications is provided by Ortega et al.[3]

Specially in highly diluted samples, XAS spectra should be of very good quality from both a statistical and spectroscopic point of view to detect weak surface changes coming from a small fraction of the sample.[4] In these cases, the conventional XAS experiment in absorption/transmission mode is not an option, as an optimal

Highlights in this review are: Combination of Imaging micro- X-ray Fluorescence spectroscopy (XRF) with XAS, by selecting multiple energies (ME); Total reflection XRF – XAS (TXRF-XAS); High energy resolution fluorescence detection XAS (HERFD-XAS) and resonant X-ray emission spectroscopy (RXES); Time resolved XAS (Quick-XAS, Dispersive-XAS, Ultrafast-XAS).

absorption edge jump is not possible to achieve. However, XAS can be performed in florescence mode, where typically energy dispersive element(s) are used. This is required to distinguish the desired X-ray photons from the ones that demean the signal-to-noise ratio. As literature shows, XAS for biological systems is used in fluorescence mode. In this mode there are several variations, developed for different levels of sensitivity: oxidations state, local coordination environment, electronic properties, spin states, and density of states.[5]

XAS requires a high flux beam, which is why it is mainly found at synchrotron sources, and X-rays have high penetration depth. This allows undertaking *in situ* experiments, with direct observation of the species at the molecular level under conditions maximum close to physiological, as mentioned by Yalovega and Kremennaya,[1] as well as Czapla-Masztafiak et al.[6] And in most of the cases without the need for preconcentration. This includes simple systems and more complex one, such as cells and tissues. In 2018 Francesco Porcaro et al. published a review on the advances in element speciation analysis of biomedical samples using synchrotron-based techniques.[7] The authors provide an overview between 2012 and 2017 with applications in pharmacology, metals and nanoparticles toxicology and physiopathology; referring to XAS as method for direct element speciation; the limitations of bulk- and micro-XAS; and future direction and developments of XAS speciation in biomedical research. Also a must read in the field of elemental and chemically Specific X-ray Fluorescence Imaging of Biological Systems is the review article from 2014 of Pushie et al.[8] Yet still valid in many current applications, they present a review of X-ray fluorescence imaging (XFI) in the hard X-ray regime (≥2 keV). They also provide an overview on XRF with micro focused X-ray beams, as well as methods that confer chemical selectivity or 3D visualization.

Biological samples remain one of the most challenging materials when it comes to studies involving X-ray based techniques. Low concentration of analyzed analyte (≤μg/g), or susceptibility to radiation damage have triggered a higher analytical sensitivity and care when it comes to conduct analyses on these samples. These factors are addressed in several studies and publications, with the use of synchrotron-based techniques. George et al[9] review the origins of photo-reduction and photo-oxidation, the impact that they can have on active site structure, and the methods that can be used to provide relief from X-ray-induced photo-chemical artifacts. One way of conveying the problem of photo-reduction or photo-oxidation is to perform the experiments under cryogenic conditions for preserving both chemical and morphological structures.[7] Garman and Weik published an overview of the recent progress on X-ray radiation damage to biological samples.[10]

The rapid (further-) development of these techniques over the past decades have opened a new window of possibilities for biological and biomedical studies. New generation X-ray sources with high intensity, unprecedented sub-μm and nm beam size, and higher energy resolution have tackled problems with signal-to-noise ratio, inherent to these types of samples. In addition, the support of theoretical calculations, whether XAS spectra or the use of classical molecular mechanics/dynamics (MM/MD) is mandatory in many cases to verify the accuracy of structure data obtained by experimental methods.[11–14]

For significantly improved signal-to-noise ratio for studying biological systems, methods providing high energy resolution fluorescence detected XAS (HERFD-XAS) are constantly gaining importance.[15–18] In cases where the analyte concentration is extremely low, in nanogram or even picogram range, the use of total reflection X-ray fluorescence XAS (TXRF-XAS) is the variant of choice.[19]

Also relevant in the field of biological systems is the advent of X-ray free electron lasers (XFELs) producing ultrashort intense X-ray pulses (pulse widths <100 fs). Measurements in the sub-picosecond timescale become available. In addition, the biggest advantage is the fact that radiation damage can be outrun and data can be collected even at room temperature.[20]

This manuscript reviews the latest analytical developments and advances in XAS, as an analytical tool for biological and biomedical applications, in the last 5 years. Specific applications will be referred but the aim hereby is to highlight the newest XAS modalities for this field of application, as shortly numerated above.

2 | MODUS OPERANDI AND APPLICATIONS

X-ray spectroscopy for speciation and probing detailed information on the electronic properties can be divided into two main groups: XAS and XES. Owing to continuous further development of several modalities, these are indeed methods of modern spectroscopy. XAS and XES, due to their complementary nature, deliver detailed information about the local electronic structure. XAS probes the transition of electrons into empty states and XES is related to the decay of electrons from upper occupied states. A short description of the various XAS and XES modii is herein provided in form of Table 1. Further details of each of the modalities and their capabilities can be found in several publications; Zimmermann et al provide a recent overview of the methods.[21] The manuscript

TABLE 1 Summary of XAS and XES modii for modern X-ray spectroscopy

Method		Modii	Features/notes
XAS Sensitive to oxidation state, qualitative and quantitative information on local geometry al structure (bond distances, coordination numbers, and disorder).	Transmission	Dispersive-XAS	Polychromatic beam interacts with the sample. Homogeneity plays a strong role: Sample preparation is required and if not possible, local densities can be averaged out by continues samples movement (faster that acquisition time). Suitable for time-resolved *in situ* studies in the range of seconds.
		Quick-XAS	Monochromatic beam scanned in offering time resolution between 10–200 milliseconds. Sample homogeneity is recommended.
		Ultrafast-XAS	At FELs: Time resolution in sub-picosecond range; radiation damage outran.
	Fluorescence	HERFD-XAS	Monochromatic beam scanned, combined with high resolution detection. Fluorescent line is monitored with a crystal analyzer, with resolution higher than the lifetime of the probed line. Sample homogeneity is not required. Suitable for low concentration samples.
XES/RXES/RIXS The kβ line holds information to the metal spin state as well as the metal–ligand covalence; the $k\beta_{2,5}$ line area is more sensitive to the ligands type, electronic structure, and metal–ligand bond length.	Fluorescence	VtC	Monochromatic beam at fixed energy (non-resonant): • Crystals analyzers are swept over the VtC emission energy range. • Dispersive mode with bent crystal. Sample homogeneity is not required. Suitable for low concentration samples
	Fluorescence	Ultrafast-XAS	At FELs: Time resolution in sub-picosecond range; radiation damage outran.

Abbreviations: RIXS, resonant inelastic X-ray scattering; RXES, resonant X-ray emission spectroscopy; XAS, X-ray absorption spectroscopy; XES, X-ray emission spectroscopy.

of Groot is a good reference for the fundamentals of these techniques[22] and the one from Bauer entails details on the high energy resolution variants.[23]

2.1 | Micro-XAS and multiple energy micro-XRF combined with micro-XAS

Spatially resolved elemental and speciation information remain one of the most used analytical approaches for studying biological samples. The most recuring methods are the scanning mode[24–26] or the full-field mode.[27,28] In both cases a micro sized X-ray beam is typically required. For this purpose, X-ray optics are used; these can be compound refractive lens (CRL), polycapillary optics, or even Kirkpatrick-Baez (K-B) mirrors.[29]

Some recent examples of applications are herein reviewed:

1. The chemical speciation of micro-nanoparticles in inflamed tissue adjacent to titanium and ceramic dental implants.[26] In this work the authors perform μ-XANES analyses on previously located higher Ti concentration spots, revealed two different chemistries. Beam size was 0.4 x 0.8 μm obtained by a KB mirror. The scans were collected by an energy dispersive SDD.
2. Distribution of metals containing particles from tattoo needle wear in humans.[25] The authors draw attention to possible allergic reactions linked to metals such as Nickel and Chromium and analyzed tattoo particles in human skin and lymph node sections by means of nano-XANES. Special attention as given to regions with Ti-containing ink. Ti was found to derive from TiO2, in a mixture of anatase and rutile, which promotes abrasion from the tattoo needle.
3. Characterization of arsenic in dried baby shrimp, as human exposure to toxic metals/metalloids among the ethnic Chinese community in Upstate New York.[27] The authors draw attention to the toxicology aspect, not just being a question of concentration but also of the species. Arsenic species was investigated by micro-XANES. Results suggest As in these shrimp samples is consistent with the organoarsenic species AsB and/or

AsC. The elemental distribution was obtained by a Maia detector, also aided to the XANES profile identification.

In terms novel analytical approaches two examples are discussed. The work from Farfan et al[30] describes a new approach combining X-ray fluorescence (XRF) and XAS for microscale imaging applied to identification of sulfur species within tissues and skeletons of Corals. The main challenge is imaging sulfur (a low Z element) in a complex matrix, which is key in understanding the distribution of biomolecules within environmental and biological systems. The authors go beyond the standard single-point XAS spectroscopy. As also found in other studies, the idea is to quantify to which extent each of the measured species plays a role in the coral and where it is distributed, by visual correlations. By overlying micro-XRF maps acquired at two single energies, that reveal the reduced and oxidized species, a fast recognition of the distribution of these phases is achieved. This approach, multiple energy (ME) μ-XRF, combined with extensive XANES points renders high-resolution spatially resolved maps of specific sulfur species. The X-ray beam was focused down to a 5 x 5 μm size by K-B mirrors. First S K-edge XANES spectra were collected between 2,460 and 2,536 eV and then XRF mappings were obtained at multiple energies (2,472.8, 2,473.9, 2,475.1, 2,476.4, 2,481.4, 2,482.4, and 2,484.7 eV) that reveal differences in the fine structure. Farfan et al show the feasibility of a stack of ME maps fitted S K-edge XANES spectra, which is useful to provide a more accurate distribution of each sulfur standard. This way, several representative absorption features are considered, rather that only one dominant XRF peak. This eliminates false peak assignation due to overlapping XRF signals. The fitting of the ME maps with XANES for sulfur was carried out by combining principal component analysis (PCA) and linear combination fitting of XANES spectra. Further insight on the procedure steps can be found in the manuscript.[30] Fitted ME micro-XRF maps of sulfur species distributions are displayed as tricolor plots, which enabled the identification of glutathione disulfide, cysteine, sulfoxide, and organic sulfate, as major sulfur components within the tissue.

A second example is the work from Liu et al.[31] This study reports on a method for redox mapping by confocal micro-XRF imaging using chromium species in a biochar particle. This approach is an extension of the one previously described, with extra depth resolved information. In this work the authors combine the advantages of full-field XANES, also exploited elsewhere,[32,33] with confocal micro-Xray fluorescence imaging. This renders elemental distributions, and hence chemical speciation along the cross section on various samples, without any previous preparation.

In sum, this ME micro-XRF in combination with LFC micro-XANES enhances the information on the distribution of different species. In this way, a much faster speciation recognition rather than in single point XAS spectroscopy is achieved. This lowers the probability of radiation damage, especially important for the investigation of biological samples {CE: Please raise an AQ.}.

2.2 | Total external reflection XAS

When performing XAS, one of the strongest limitations is the interference of other interaction of X-rays and matter that take place simultaneously. One of them is X-ray scattering, which is the main physical factor determining detection limits (DL) of trace elements. These effects play even a stronger role when studying biological related materials. Gherase and Fleming discuss such limitations and challenges in a recent an overview probing trace elements in human tissue with synchrotron radiation.[34] Total external reflection XAS (TXRF-XAS) remains the method of choice for probing chemical species on ultra-low concentrations of analyte/probed element. The feasibility of this method for biological samples has been proven in the past by Meirer et al.[35] The combination of TXRF and XAS was applied for arsenic speciation (AsIII and AsV) in xylem sap of cucumber plants, with very good DLs of As (170 $ng.l^{-1}$). At grazing angles below the critical angle θc, X-rays are mostly total reflected. This drastically reduces the probability of scattering events and, consequently, improves elemental DL in the nanogram/gram or picogram/gram region. θc is inversely proportional to photon energy; hence the geometrical constraints imposed by the very small critical angle have limited TXRF-XAS applications to probing elemental composition of small samples or with very smooth surfaces. Further technical insight on TXRF principles can be found elsewhere by Wobrauschek.[36]

There are several beamlines beamlines worldwide that provide TXRF measurements. An overview of these beamlines with technical specifications is given by Streli et al.[37] Except for the beamline L at the HASYLAB, all other beamlines are still active. The automatic sample changer chamber for TXRF-XAS analysis developed for Beamline L is now available at the BAM*line* at BESSY-II.[19]

2.3 | High energy resolution fluorescence detection XAS and resonant X-ray emission spectroscopy

Literature research reveals a constant increase of HERFD-XAS and RXES in the field of biological and

biomedical applications. These methods enable significantly improved signal-to-noise ratios, which is a premise for analyzing biological systems. The sharp and well-marked features of the spectra obtained in this manner enable to determine unambiguously and with greater precision the speciation and electronic structure of the probed elements. When performing X-ray spectroscopy measurements in fluorescence with XAS information, we can distinguish HERFD-XAS and X-ray emission spectroscopy (XES), K- and L- level X-ray emission spectra, reflect the energy distribution of photons emitted by the atoms, which can be divided into α and β regions. Although α lines have high transition yields they provide little chemical information. However, β lines—linked to satellite lines—are far more sensitive to the chemical environment in the vicinity of the atom. The problem is that these are much weaker in intensity, which presents a challenge in detection. In this context, two areas can be distinguished in the XES spectrum of a kβ-line: the main transition (kβ line) resulting from the transition 3p to 1 s in the metal state and the valence-to-core (VtC) transition (kβ2,5 line), resulting of transitions from valence states into metal state 1 s, as the name says. The kβ line holds information to the metal spin state as well as the metal–ligand covalence; the kβ2,5 line (or VtC area) is more sensitive to the ligands type, electronic structure, and metal–ligand bond length.[6,38] Further details of XES theories and core-level spectroscopy can be found elsewhere[23,39–41] .

This detailed chemical information is conducted using HERFD spectrometers, obtained by REXS, also known as resonant inelastic X-ray scattering. These are so-called photon-in photon-out spectroscopies, obtained by wavelength dispersive spectrometers. This is achieved by dispersion of X-rays with a crystal analyzer (CA) with high intrinsic energy resolution. Ideally with higher resolution than the natural width of the probed line, which for most cases it falls in the region between 0.1 and 3 eV. There are three relevant XES spectrometer geometries: von Hamos, Johannson, and Johann.[6] Figure 1 shows an example of setup for XAS-fluorescence measurement using solid-state detector (SSD) and crystal analyzer spectrometer (CAS) in high resolution mode (HERFD). The spectra correspond to the analysis of a Co3O4 sample with a 30-element Ge SSD (total fluorescence yield) and a CAS using five Ge(444) crystals optimized around the Co Kβ1,3 fluorescence line (HERFD). Also here further technical details on the geometry used for the XES experiment can be further studied in Proux et al.[4]

A few recent applications using HERFD-XAS are reviewed.

One example is published by Bissardon et al,[15] taking advantage of a CAS spectrometer for high energy resolved XAS studies of selenium (Se) on articular

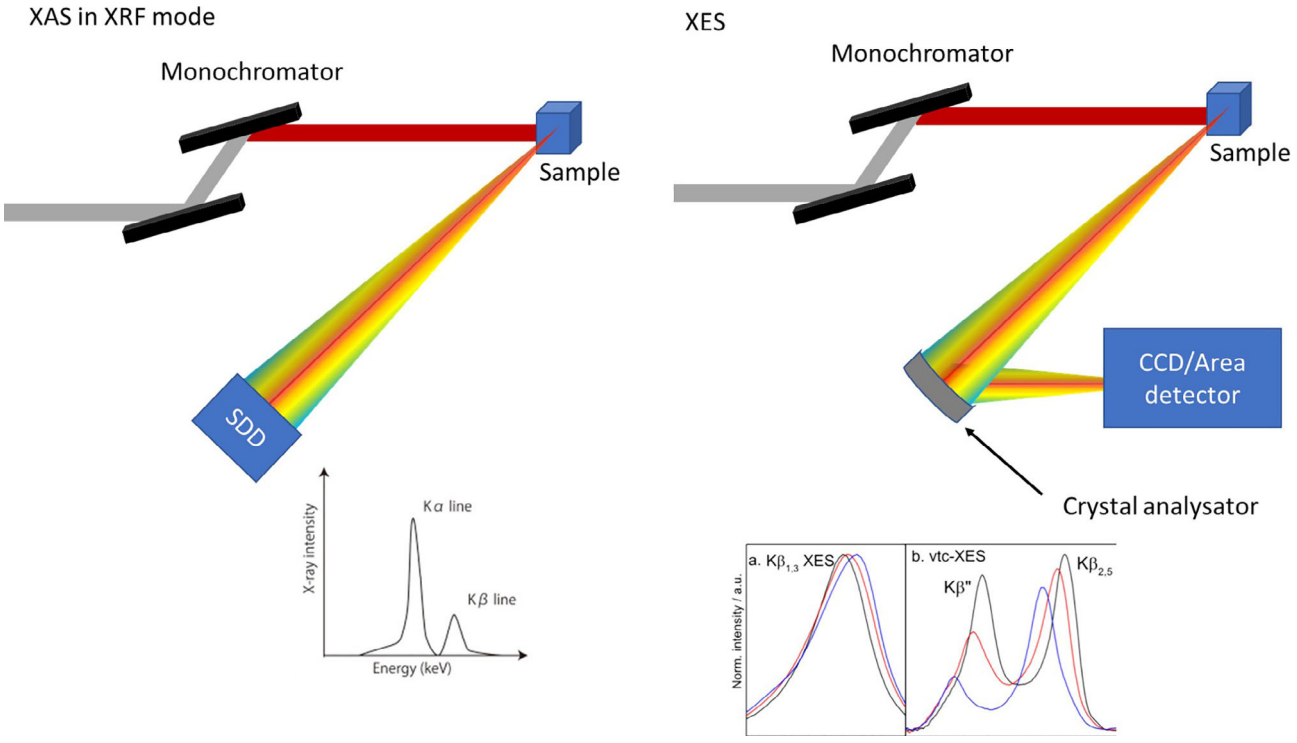

FIGURE 1 XAS principles in XRF mode (left) and XES (right). XAS, X-ray absorption spectroscopy; XRF, X-ray fluorescence spectroscopy

cartilage. Se concentrations in cell tissue are typically in the low ppb range (μg/kg). In this case, lowering the DL of XAS for speciation purposes is mandatory. The authors report on a wavelength dispersed spectrometer in a Johan geometry to perform speciation in 400 ppb of Se. This represents a huge analytical advance in the realm of direct speciation with X-rays on highly diluted systems through XAS {CE: Please raise an AQ.}. With this technique, new possibilities are presented to study, for example, the metabolic role of Se and other elements in biological samples. The importance of Se remains unquestioned in human health—in biological activities and toxic effects that depend not only on the concentration but also on the chemical species. In addition, and to preserve the chemical species within the samples, the measurements were performed in cryogenic conditions, with a He flow cryostat. This way radiation damage is reduced. The study involved determining the major species present in bovine articular cartilage during an accelerated maturation process. The samples were snap-frozen in precooled hexane and cryo-milled to obtain a homogeneous fine powder that was transferred under anoxic conditions to a He-cryostat for HERFD-XAS. Further analytical details on sample preparation and conduction of the measurements can be found in the manuscript.[15]

Further examples of XES in higher resolution mode applied to investigate zinc (Zn), as the second most common transition metals in the human body, are presented by McCubbin et al[42] and Thomas et al.[17] In both studies, the importance of Zn is undoubtable but it has few viable routes for its direct

structural study in biological systems. The former makes use of VtC XES and XAS at the Zn K-edge to understand the local structure of Zn in a series of biologically relevant molecular model complexes.

The viability of these spectroscopic methods was assessed by analyzing these complexes, specifically the bond zinc-to-oxygen, -nitrogen, and -sulfur. The chosen ligands exhibit similarity to relevant aminoacids: benzoate (BzO) to mimic aspartate/glutamate, 1-methylimidazole (MeIm) and 2-aminopyridine (pyNH2) for histidine, and thiourea (SC [NH2]2) and thiophenol (SPh) for cysteine. In order to gain insight on the local coordination geometry and how this influences the absorption and emission spectra, two complexes were also investigated: [Zn(MeIm)6]2+ and [Zn (MeIm)4]2+. A deeper understanding of the experimentally observed features, density functional theory (DFT) based on spectra calculations was carried out. This complementarity of both spectroscopies and theory represents a current trend and allows future applications to protein systems in a predictive manner.[42]

The latter shows a study of Zn coordination in biological samples, retrieved by HERFD-XAS, enhancing the fact that this method allows identification of near-Z neighboring atoms (e.g., O and N), which is a challenge for EXAFS in its standard mode. In this study, the authors performed direct determination of Zn ligation in whole cell bacteria, revealing coordination to carboxyl, phosphoryl, imidazole, and/or thiol moieties in model microorganisms unambiguously.[17]

Another example that combines HERFD-XAS, VtC-XES both experimentally and theoretically is given by Müller et al.[16] The goal was to investigate complexes that mimic biologically important Cu_A site. For this purpose, three selected complexes of type [Cu2(NGuaS)2X2] were carried out. They were characterized by a cyclic Cu2S2 core portion and a varying adjunct ligand nature. The combination of HERFD-XANES, VtC-XES with extensive DFT calculations could reveal details on the electronic states, including HUMO and LUMO levels and spin states. The value of this experiment/theory combination remains unquestionable for further *in situ* studies.[16]

2.4 | Time resolved XAS/XES (quick-XAS, dispersive-XAS, ultrafast-XAS)

With the advent of extremely high brilliant sources for example, at new generation synchrotron or X-ray free electron lasers (XFELs) facilities, time-resolved studies on highly diluted systems (such as biological samples) become feasible with unprecedent signal-to-noise ratios.

Among the time resolved XAS methods, Quick-XAS and Dispersive-XAS are the most found at synchrotron facilities. Quick-XAS has replaced the step-by-step acquisition of every energy point by continuously scanning the whole XAS spectrum.[43] The monochromator movement is triggered by a piezo motorized stage with a frequency between 50 and 70 Hz. This allows a whole XAS spectrum (XANES+EXAFS) to be measured between 10 and 200 ms.[44–46]

An example where Quick-XAS was employed is given by Zheng et al,[47] where the authors investigate Selenocompounds (SeCs). SeCs are categorized as promising therapeutic agents for a wide range of diseases including cancer. What makes these compounds interesting spectroscopically, is that the treatment results depend on both the chemical species and the concentration. Again, we are faced with the challenge of dilution and possible radiation damage. To understand the mechanisms underlying the heterogeneous cytotoxicity of SeCs, the authors investigated selenium speciation of SeCs representing different categories using liquid chromatography-mass spectrometry (LC–MS) and Quick-XAS. Se K-edge XAS measurements were performed in Quick-XAS mode using a Si(311) double-crystal

monochromator in CLAESS beamline at ALBA synchrotron light facility (Barcelona, Spain).[48]

To avoid radiation damage, all measurements were performed at liquid N2 temperature using the cryostat available at the beamline. The analysis corroborated the covalent binding between selenol.

intermediates of SeCs and albumin thiols. For the first time, the Se-S model could be profiled for four SeCs. And also for the first time it was observed that cytotoxic SeCs could spontaneously transform into selenol intermediates that immediately react with albumin thiols through Se-S bond.[47]

The other approach is dispersive-XAS, which consists of diffraction a polychromatic beam—of a specific bandwidth—by a bent crystal (e.g., Si 111). Numerous studies have been performed with the aim of improving the performance of these setups for different applications.[49–52] In dispersive-XAS there is no scanning involved, as the whole polychromatic beam interacts with the sample and is then diffracted by a crystal. This results in more beam position stability. However, the time resolution is in the sub-second range. The detection system functions often as area sensitive detectors (or position sensitive detectors), such as CCD-based detectors. A fast readout low noise CCD camera (FReLoN) was developed at the European Synchrotron Radiation Facility (ESRF). The FReLoN enables 20 frames per second. Nowadays, a beam size of 5 μm × 5 μm with a time resolution of about 60 ms can be achieved.[53] For time resolved studies on samples with biological interest that fall in the second time frame, dispersive XAS is the choice.

The dispersive-XAS setup available at the BAM*line* is displayed in Figure 2 left hand-side. Contrary to all other dispersive-XAS setups, the sample is placed before the dispersive element (crystal analyser Si 111), in X-rays upstream. This is an advantage because just the X-rays-that contribute to the XAS region are diffracted and no scattering is included in the resulting picture on the CCD camera. The whole XAS spectrum is acquired in a single shot, owed to the bending of the Si 111. This and a simple θ-2θ geometry are enough requirements for a simple scanningless dispersive-XAS setup.[50,51] One example of application to samples with biological interest is displayed in Figure 2, right-hand side.

In this study, the early stages of ZIF-8 crystallization were investigated by dispersive-XAS.[54] This provided an understanding of the evolution of the coordination environment in the vicinity of Zn during crystallization. Linear combination fitting suggests tetrakis(1-methylimidazole) zinc2+ to be a suitable and stable mononuclear. This is the first step into more detailed physico-chemical aspects of ZIF-8 crystallization, aiming at better control tailoring ZIF-8 materials for specific applications. ZIF-8 and its analogues have been studied for a variety of applications. These include drug delivery vehicle, and carrier for biomacromolecules.[54]

XFELs produce ultrashort intense X-ray pulses (<100 fs), which enables experiments in the sub-picosecond

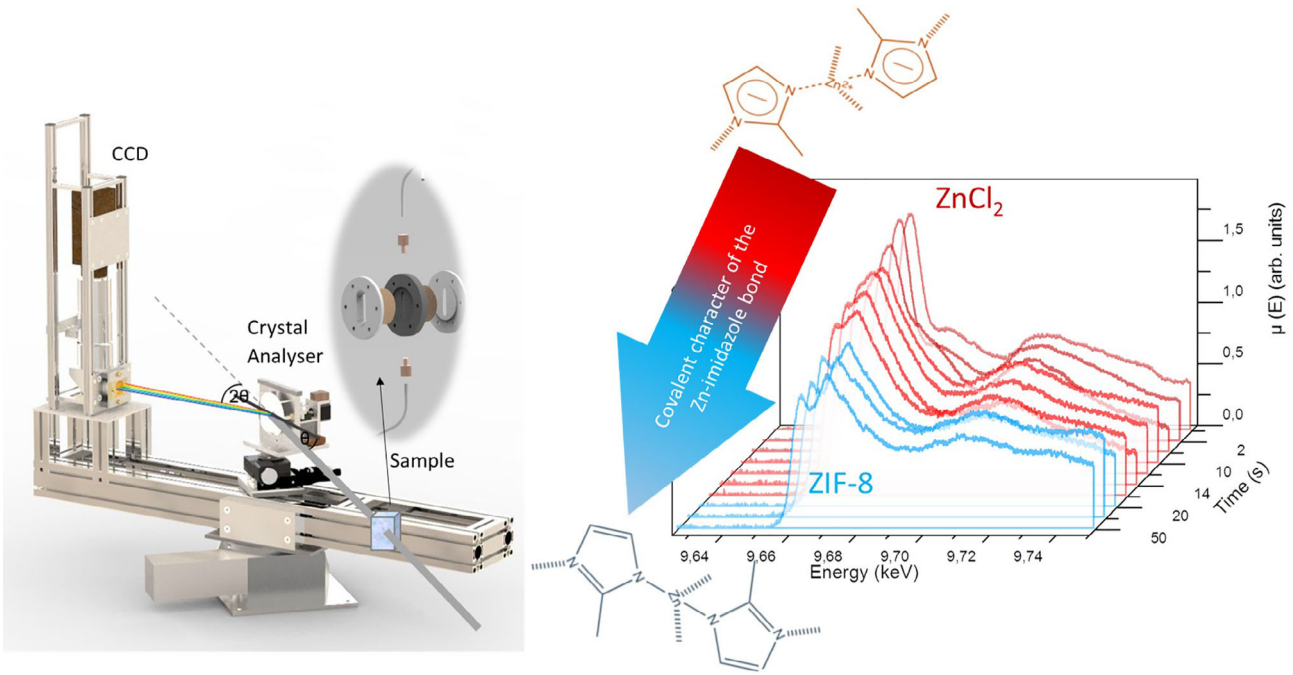

FIGURE 2 Left: experimental setup for dispersive-X-ray absorption spectroscopy measurements available at the BAM*line*; right-hand side: *in situ* study on the crystallization process of ZIF-8 with time resolution of 1 second

range and outrun radiation damage. Together with a peak brilliance of several orders of magnitude higher than in synchrotron facilities, it is advantageous for time-resolved XAS and RXES experiments on biological samples at room temperature.[20]

Chatterjee et al[20] demonstrate that Mn K-edge XAS of solutions with millimolar concentrations of metal is possible using the femtosecond X-ray pulses from XFELs. The measurements were carried out at the X-ray pump and probe end-station of the Linac coherent light source.[55] An X-ray beam with a pulse length of ~40 fs and a 2 x 10^{12} to 3 x 10^{12} photons per pulse was used, at a repetition rate of 120 Hz. The data were collected using two modes: Rayleigh jet, and drop-on-demand, with varying Mn concentrations. Mn XAS spectra were collected in fluorescence using an ePix-100 detector with 768 x 704 pixels[56] at an angle of 90° with respect to the beam to minimize scattering.

Both XANES and EXAFS spectra of such dilute solution samples are in good agreement with data collected at synchrotron sources using traditional scanning protocols. The procedures described here will enable XFEL-based XAS on dilute biological samples, especially metalloproteins, with low sample consumption.[55]

One concrete example of the use of polarized-XAS is shown by Miller et al.[57] This ultrafast, polarization-selective time-resolved XANES is used to characterize the photochemistry of vitamin B12, cyanocobalamin (CNCbl), in solution. Cobalamins are important biological cofactors involved many biological processes. Time-resolved polarized XAS provides a powerful tool for unraveling structural transformations in isotropic systems. The results reported by Miller et al[57] exploit the in-plane polarization of the lowest absorption band of CNCbl. The results reveal features that influence the reactivity and deactivation of electronically excited cobalmins, supported by simulations. This is big step forward for the applicability of ultrafast polarized XANES technique to any system where a well-defined molecular excitation direction can be identified.

3 | CONCLUSIONS AND OUTLOOK

The latest analytical developments for probing biological and biomedical systems with XAS have been reviewed. The rapid development of synchrotron- and XFEL-based methods for XAS techniques have open a new window of opportunities for the characterization of challenging biological samples. The main challenges are (extremely) low concentration of analyte and susceptibility for radiation damage.

Unprecedented micro- and sub-micrometer sized X-ray beams together with fast (and ultrafast) measurement times, have promoted XAS to a method of choice for characterizing this kind of samples.

The analytical developments fall into higher sensitivity (higher DL)—such as TXRF-XAS or HERFD-XAS and RXES; combining other techniques to exploit the chemical information of the sample—this is the case of imaging micro-XRF with -XAS selecting ME; or by time resolved spectroscopies, such as Quick-XAS, Dispersive-XAS or ultrafast-XAS at XFELs).

A trend observed is the support of theoretical calculations, whether XAS spectra or the use of classical molecular mechanics/dynamics (MM/MD) to verify the accuracy of structure data obtained by experimental methods. DFT/MD will become part of experimental investigations to fully describe electronic properties, local structure, and other spectroscopic features in the realm of X-ray absorption spectroscopy.

ORCID

Ana Guilherme Buzanich https://orcid.org/0000-0001-5543-9924

REFERENCES

[1] G. E. Yalovega, M. A. Kremennaya, *Crystallogr. Rep.* **2020**, *65*, 813. https://doi.org/10.1134/s1063774520060395.

[2] J. F. Collingwood, F. Adams, *Spectrochim. Acta. B At Spectrosc.* **2017**, *130*, 101. https://doi.org/10.1016/j.sab.2017.02.013.

[3] R. Ortega, A. Carmona, I. Llorens, P. L. Solari, *J. Anal. At Spectrom.* **2012**, *27*, 2054. http://doi.org/10.1039/c2ja30224a.

[4] O. Proux, E. Lahera, W. Del Net, I. Kieffer, M. Rovezzi, D. Testemale, M. Irar, S. Thomas, A. Aguilar-Tapia, E. F. Bazarkina, A. Prat, M. Tella, M. Auffan, J. Rose, J. L. Hazemann, *J. Environ. Qual.* **2017**, *46*, 1146. https://doi.org/10.2134/jeq2017.01.0023.

[5] G. Bunker, *Introduction to XAFS: A Practical Guide to X-Ray Absorption Fine Structure Spectroscopy*, Cambridge University Press, Cambridge **2010**.

[6] J. Czapla-Masztafiak, W. M. Kwiatek, J. Sá, J. Szlachetko, in *XRay Spectroscopy on Biological Systems. X-ray Scattering* (Ed: A. E. Ares), IntechOpen, UK **2017**, p. 183. https://www.intechopen.com/books/x-ray-scattering/x-ray-spectroscopy-onbiological-systems.

[7] F. Porcaro, S. Roudeau, A. Carmona, R. Ortega, *TrAC Trends Anal. Chem.* **2018**, *104*, 22. http://doi.org/10.1016/j.trac.2017.09.016.

[8] M. J. Pushie, I. J. Pickering, M. Korbas, M. J. Hackett, G. N. George, *Chem. Rev.* **2014**, *114*, 8499. https://doi.org/10.1021/cr4007297.

[9] G. N. George, I. J. Pickering, M. J. Pushie, K. Nienaber, M. J. Hackett, I. Ascone, B. Hedman, K. O. Hodgson, J. B. Aitken, A. Levina, C. Glover, P. A. Lay, *J. Synchrotron Radiat.* **2012**, *19*, 875. https://doi.org/10.1107/s090904951203943x.

[10] E. F. Garman, M. Weik, *J. Synchrotron Radiat.* **2019**, *26*, 907. https://doi.org/10.1107/s1600577519009408.

[11] M. Anselmi, N. Sanna, C. Padrin, L. Balducci, M. Cammarata, E. Pace, M. Chergui, M. Benfatto, *Struct. Dyn.* **2018**, *5*, 054101. https://doi.org/10.1063/1.5031806.

[12] A. Maire du Poset, A. Zitolo, F. Cousin, A. Assifaoui, A. Lerbret, *Phys. Chem. Chem. Phys.* **2020**, *22*, 2963. https://doi.org/10.1039/c9cp04065j.

[13] M. Ross, A. Andersen, Z. W. Fox, Y. Zhang, K. Hong, J. H. Lee, A. Cordones, A. M. March, G. Doumy, S. H. Southworth, M. A. Marcus, R. W. Schoenlein, S. Mukamel, N. Govind, M. Khalil, *J. Phys. Chem. B* **2018**, *122*, 5075. http://doi.org/10.1021/acs.jpcb.7b12532.

[14] A. G. Walsh, Z. Chen, P. Zhang, *J. Phys. Chem. C* **2020**, *124*, 4339. http://doi.org/10.1021/acs.jpcc.9b09548.

[15] C. Bissardon, O. Proux, S. Bureau, E. Suess, L. H. E. Winkel, R. S. Conlan, L. W. Francis, I. M. Khan, L. Charlet, J. L. Hazemann, S. Bohic, *Analyst.* **2019**, *144*, 3488. http://doi.org/10.1039/c9an00207c.

[16] P. Müller, A. Neuba, U. Flörke, G. Henkel, T. D. Kühne, M. Bauer, *J. Phys. Chem. A* **2019**, *123*, 3575. http://doi.org/10.1021/acs.jpca.9b00463.

[17] S. A. Thomas, B. Mishra, S. C. B. Myneni, *J. Phys. Chem. Lett.* **2019**, *10*, 2585. http://doi.org/10.1021/acs.jpclett.9b01186.

[18] M.-P. Isaure, M. Albertelli, I. Kieffer, R. Tucoulou, M. Petrel, E. Gontier, E. Tessier, M. Monperrus, M. Goñi-Urriza, *Front Microbiol.* **2020**, *11*. http://doi.org/10.3389/fmicb.2020.584715.

[19] U. Fittschen, A. Guilherme, S. Böttger, D. Rosenberg, M. Menzel, W. Jansen, M. Busker, Z. P. Gotlib, M. Radtke, H. Riesemeier, P. Wobrauschek, C. Streli, *J. Synchrotron Radiat.* **2016**, *23*, 820. http://doi.org/10.1107/s1600577516001995.

[20] R. Chatterjee, C. Weninger, A. Loukianov, S. Gul, F. D. Fuller, M. H. Cheah, T. Fransson, C. C. Pham, S. Nelson, S. Song, A. Britz, J. Messinger, U. Bergmann, R. Alonso-Mori, V. K. Yachandra, J. Kern, J. Yano, *J. Synchrotron Radiat.* **2019**, *26*, 1716. http://doi.org/10.1107/s1600577519007550.

[21] P. Zimmermann, S. Peredkov, P. M. Abdala, S. DeBeer, M. Tromp, C. Müller, J. A. van Bokhoven, *Coord. Chem. Rev.* **2020**, *423*, 213466. http://doi.org/10.1016/j.ccr.2020.213466.

[22] F. de Groot, *Chem. Rev.* **2001**, *101*, 1779. http://doi.org/10.1021/cr9900681.

[23] M. Bauer, *Phys. Chem. Chem. Phys.* **2014**, *16*, 13827. http://doi.org/10.1039/c4cp00904e.

[24] O. Hachmöller, A. G. Buzanich, M. Aichler, M. Radtke, D. Dietrich, K. Schwamborn, L. Lutz, M. Werner, M. Sperling, A. Walch, U. Karst, *Metallomics.* **2016**, *8*, 648. http://doi.org/10.1039/c6mt00001k.

[25] I. Schreiver, B. Hesse, C. Seim, H. Castillo-Michel, L. Anklamm, J. Villanova, N. Dreiack, A. Lagrange, R. Penning, C. De Cuyper, R. Tucoulou, W. Bäumler, M. Cotte, A. Luch, *Part Fibre. Toxicol.* **2019**, *16*. http://doi.org/10.1186/s12989-019-0317-1.

[26] K. Nelson, B. Hesse, O. Addison, A. P. Morrell, C. Gross, A. Lagrange, V. I. Suarez, R. Kohal, T. Fretwurst, *Anal. Chem.* **2020**, *92*, 14432. http://doi.org/10.1021/acs.analchem.0c02416.

[27] D. Guimarães, A. A. Roberts, M. W. Tehrani, R. Huang, L. Smieska, A. R. Woll, S. Lin, P. J. Parsons, *J. Anal. At Spectrom.* **2018**, *33*, 1616. http://doi.org/10.1039/c8ja00094h.

[28] U. Boesenberg, C. G. Ryan, R. Kirkham, A. Jahn, A. Madsen, G. Moorhead, G. Falkenberg, J. Garrevoet, *J. Synchrotron Radiat.* **2018**, *25*, 892. http://doi.org/10.1107/s1600577518004940.

[29] A. Guilherme, G. Buzanich, M. L. Carvalho, *Spectrochim. Acta B. At Spectrosc.* **2012**, *77*, 1. http://doi.org/10.1016/j.sab.2012.07.021.

[30] G. A. Farfan, A. Apprill, S. M. Webb, C. M. Hansel, *Anal. Chem.* **2018**, *90*, 12559. http://doi.org/10.1021/acs.analchem.8b02638.

[31] P. Liu, C. J. Ptacek, D. W. Blowes, Y. Z. Finfrock, M. Steinepreis, F. Budimir, *Anal. Chem.* **2019**, *91*, 5142. http://doi.org/10.1021/acs.analchem.8b05718.

[32] F. Meirer, J. Cabana, Y. Liu, A. Mehta, J. C. Andrews, P. Pianetta, *J. Synchrotron Radiat.* **2011**, *18*, 773. http://doi.org/10.1107/s0909049511019364.

[33] P. Paleo, E. Pouyet, J. Kieffer, *J. Synchrotron Radiat.* **2014**, *21*, 456. http://doi.org/10.1107/s160057751400023x.

[34] M. R. Gherase, D. E. B. Fleming, *Crystals* **2019**, *10*, 12. http://doi.org/10.3390/cryst10010012.

[35] F. Meirer, G. Pepponi, C. Streli, P. Wobrauschek, V. G. Mihucz, G. Záray, V. Czech, J. A. C. Broekaert, U. E. A. Fittschen, G. Falkenberg, *X-Ray Spectrom.* **2007**, *36*, 408. http://doi.org/10.1002/xrs.993.

[36] P. Wobrauschek, *X-Ray Spectrom.* **2007**, *36*, 289. http://doi.org/10.1002/xrs.985.

[37] C. Streli, P. Wobrauschek, F. Meirer, G. Pepponi, *J. Anal. At Spectrom.* **2008**, *23*, 792. http://doi.org/10.1039/b719508g.

[38] M. Lundberg, T. Kroll, S. DeBeer, U. Bergmann, S. A. Wilson, P. Glatzel, D. Nordlund, B. Hedman, K. O. Hodgson, E. I. Solomon, *J. Am. Chem. Soc.* **2013**, *135*, 17121. http://doi.org/10.1021/ja408072q.

[39] S. DeBeer, U. Bergmann, X-ray emission spectroscopic techniques in bioinorganic applications. in *Encyclopedia of Inorganic and Bioinorganic Chemistry*, Wiley, Hoboken, NJ **2011**, p. 1.

[40] J. K. Kowalska, F. A. Lima, C. J. Pollock, J. A. Rees, S. DeBeer, *Israel J. Chem.* **2016**, *56*, 803. http://doi.org/10.1002/ijch.201600037.

[41] F. de Groot, A. Kotani, *Core Level Spectroscopy of Solids*, 1st ed., CRC Press, Florida **2008**.

[42] O. McCubbin Stepanic, J. Ward, J. E. Penner-Hahn, A. Deb, U. Bergmann, S. DeBeer, *Inorg. Chem.* **2020**, *59*, 13551. http://doi.org/10.1021/acs.inorgchem.0c01931.

[43] R. Frahm, M. Richwin, D. LtzenkirchenHecht, *Phys. Scr.* **2005**, 974. http://doi.org/10.1238/physica.topical.115a00974.

[44] O. Müller, M. Nachtegaal, J. Just, D. Lützenkirchen-Hecht, R. Frahm, *J. Synchrotron Radiat.* **2016**, *23*, 260. http://doi.org/10.1107/s1600577515018007.

[45] O. Müller, D. Lützenkirchen-Hecht, R. Frahm, *Rev. Sci. Instrum.* **2015**, *86*, 093905. http://doi.org/10.1063/1.4929866.

[46] O. Mathon, A. Beteva, J. Borrel, D. Bugnazet, S. Gatla, R. Hino, I. Kantor, T. Mairs, M. Munoz, S. Pasternak, F. Perrin, S. Pascarelli, *J. Synchrotron Radiat.* **2015**, *22*, 1548. http://doi.org/10.1107/s1600577515017786.

[47] W. Zheng, R. He, R. Boada, M. A. Subirana, T. Ginman, H. Ottosson, M. Valiente, Y. Zhao, M. Hassan, *Sci. Rep.* **2020**, *10*. http://doi.org/10.1038/s41598-020-57983-y.

[48] L. Simonelli, C. Marini, W. Olszewski, M. Ávila Pérez, N. Ramanan, G. Guilera, V. Cuartero, K. Klementiev, *Cogent. Phys.* **2016**, *3*. http://doi.org/10.1080/23311940.2016.1231987.

[49] S. Pascarelli, T. Neisius, S. De Panfilis, *J. Synchrotron Radiat.* **1999**, *6*, 1044. http://doi.org/10.1107/s0909049599004513.

[50] A. G. Buzanich, M. Radtke, U. Reinholz, H. Riesemeier, F. Emmerling, *J. Synchrotron Radiat.* **2016**, *23*, 769. http://doi.org/10.1107/s1600577516003969.

[51] A. Kulow, S. Witte, S. Beyer, A. Guilherme Buzanich, M. Radtke, U. Reinholz, H. Riesemeier, C. Streli, *J. Anal. At Spectrom.* **2019**, *34*, 239. http://doi.org/10.1039/c8ja00313k.

[52] D. F. Sanchez, A. S. Simionovici, L. Lemelle, V. Cuartero, O. Mathon, S. Pascarelli, A. Bonnin, R. Shapiro, K. Konhauser, D. Grolimund, P. Bleuet, *Sci. Rep.* **2017**, *7*. http://doi.org/10.1038/s41598-017-16345-x.

[53] S. Pascarelli, G. Aquilanti, G. Guilera, O. Mathon, M. A. Newton, A. Trapananti, L. Dubrovinsky, M. Munoz, M. Pasquale, *AIP Conf. Proc.* **2007**, *882*, 608.

[54] A. Guilherme Buzanich, A. Kulow, A. Kabelitz, C. Grunewald, R. Seidel, A. Chapartegui-Arias, M. Radtke, U. Reinholz, U. Emmerling, S. Beyer, *Soft. Matter.* **2021**, *17*, 331. http://doi.org/10.1039/d0sm01356k.

[55] M. Chollet, R. Alonso-Mori, M. Cammarata, D. Damiani, J. Defever, J. T. Delor, Y. Feng, J. M. Glownia, J. B. Langton, S. Nelson, K. Ramsey, A. Robert, M. Sikorski, S. Song, D. Stefanescu, V. Srinivasan, D. Zhu, H. T. Lemke, D. M. Fritz, *J. Synchrotron. Radiat.* **2015**, *22*, 503. http://doi.org/10.1107/s1600577515005135.

[56] G. Blaj, C.-E. Chang, C. J. Kenney, *AIP Conf. Proc.* **2019**, *2054*, 060077.

[57] N. A. Miller, A. Deb, R. Alonso-Mori, B. D. Garabato, J. M. Glownia, L. M. Kiefer, J. Koralek, M. Sikorski, K. G. Spears, T. E. Wiley, D. Zhu, P. M. Kozlowski, K. J. Kubarych, J. E. Penner-Hahn, R. J. Sension, *J. Am. Chem. Soc.* **2017**, *139*, 1894. http://doi.org/10.1021/jacs.6b11295.

How to cite this article: A. Guilherme Buzanich, *X-Ray Spectrom* **2021**, 1. https://doi.org/10.1002/xrs.3254